Electronic Supplementary Information

Facile, fast and green synthesis of a highly porous calcium-syringate bioMOF with intriguing triple bioactivity

Albert Rosado,*[a] Oriol Vallcorba,[b] Blanca Vázquez-Lasa,[c,d] Luis García-Fernández,[c,d] Rosa Ana Ramírez-Jiménez,[c,d] María Rosa Aguilar,[c,d] Ana M. López-Periago,[a] Concepción Domingo*[a] and José A. Ayllón*[e]

[a] Institut de Ciència de Materials de Barcelona, ICMAB-CSIC, Campus UAB s/n, 08193 Bellaterra, Spain.
Email: arosado@icmab.es, conchi@icmab.es
[b] ALBA Synchrotron Light Source, Carrer de la Llum, 2, 26, 08290 Cerdanyola del Vallés, Barcelona, Spain.
[c] Instituto de Ciencia y Tecnología de Polímeros, ICTP-CSIC, C/ Juan de la Cierva, 3, 28006 Madrid, Spain.
[d] Networking Biomedical Research Centre in Bioengineering, Biomaterials and Nanomedicine, CIBER-BBN, Av. Mon-forte de Lemos, 3-5, 28029 Madrid, Spain.
[e] Universitat Autònoma de Barcelona, UAB, Campus UAB s/n, 08193 Bellaterra, Spain.
Email: JoseAntonio.Ayllon@uab.es

Table of contents

Crystalline structure description

The crystalline structure of CaSyr-1 belongs to the trigonal system with the space group $R\bar{3}$ (Table S3). The asymmetric unit contains two crystallographically independent Ca^{2+} ions, two independent Syr^{2-} linkers and two H_2O ancillary ligands (Fig. S5). However, both Ca^{2+} ions show comparable coordination environment and both Syr^{2-} linkers play the same role in the structure (Table S4, S5). Ca1 and Ca2 display a distorted pentagonal bipyramidal geometry, with the typical heptacoordination of calcium. Ca1 and Ca2 are arranged in dimers through a double connection promoted by μ_2-oxo (O2 and O5) bridges coming from the deprotonated phenol group in Syr^{2-}. Besides, each Syr^{2-} provides two additional oxygen atoms from the methoxy groups (O1, O3 and O4, O6, respectively), one to each Ca^{2+}, reinforcing the μ_2-phenoxo bridges. To rationalize the description of the structure, it is considered that each dimeric subunit is formed by the two Ca^{2+} and the two Syr^{2-} that are held together through the methoxy-phenolate-methoxy double clamp. The pentagonal plane coordination in the coordination sphere of each calcium is completed by an oxygen (O8 and O10, respectively) coming from a carboxylate group of a syringate that participates in the formation of a neighboring dimeric subunit. Regarding the axial axis, one position is occupied by one aquo ligand (O11 and O12, respectively) and the other by another oxygen atom carboxylate (O7 and O9, respectively) coming from another close binuclear subunit. Hence, each syringate dianion participates in the formation of a dimer by the deprotonated phenol, reinforced by the two adjacent methoxide groups, while interconnecting two other dimeric units of an adjacent chain by an asymmetric μ_2-η^1: η^1 carboxylate bridge. These bridges define chains parallel to the *c* axis (Fig. S6b), and in each chain the consecutive dimers are related by a center of inversion (Fig. 5d), thus, two different inter-dimer Ca-Ca distances alternate (Ca1···Ca1, d1, and Ca2···Ca2, d2, Fig. S6a). Each chain is connected to four

neighbor chains forming two types of prisms, triangular and hexagonal (ratio 2:1) (Fig. S6c), with a disposition in the space that resembles to the Kagome lattice (Fig. S6d). The roughly triangular sections do not display useful porosity according to the measurements in Mercury using a probe radius = 1.2 Å. Contrarily, the hexagonal section displays defined channels of Ø = 14 Å that in the crystal was filled by a disordered mixture of solvents, water and DMF, one molecule of each per calcium atom, so solvent masking strategy was used to refine the crystal structure. Experimental data, particularly powder XRD and N_2 adsorption desorption characterization show that the Kagome framework remains intact after solvent elimination and gives rise to a highly porous architecture with a 36 v% of empty void per unit cell volume.

Figures

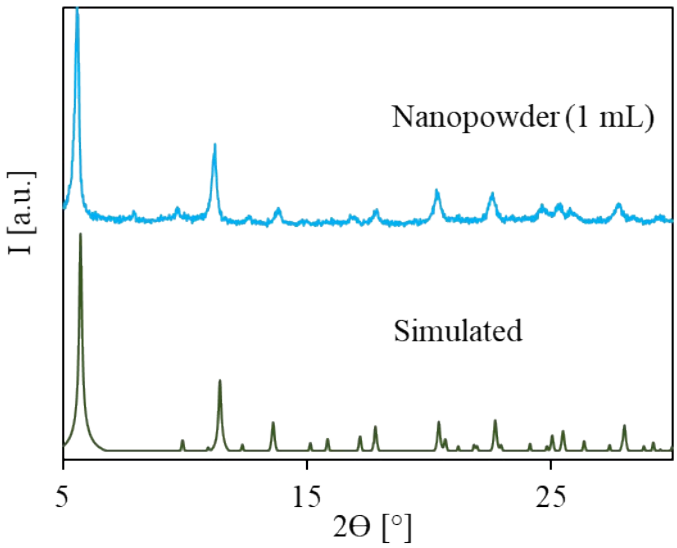

Figure S1. PXRD pattern of CaSyr-1 nanopowder prepared in 1 mL of EtOH (1:8 reactants:solvent molar ratio) compared with the simulated pattern from single crystal structural data.

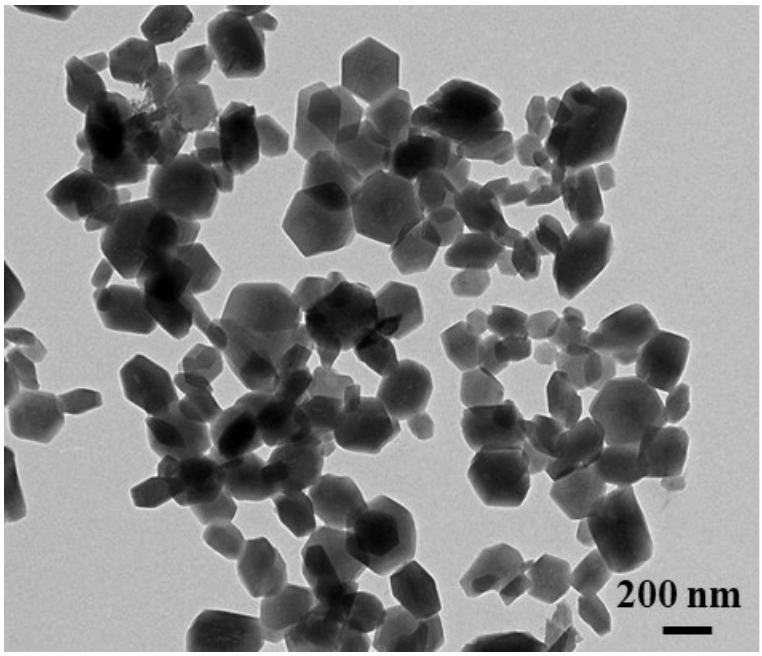

Figure S2. TEM image of CaSyr-1 nanopowder prepared in 1 mL of EtOH (1:8 reactants:solvent molar ratio).

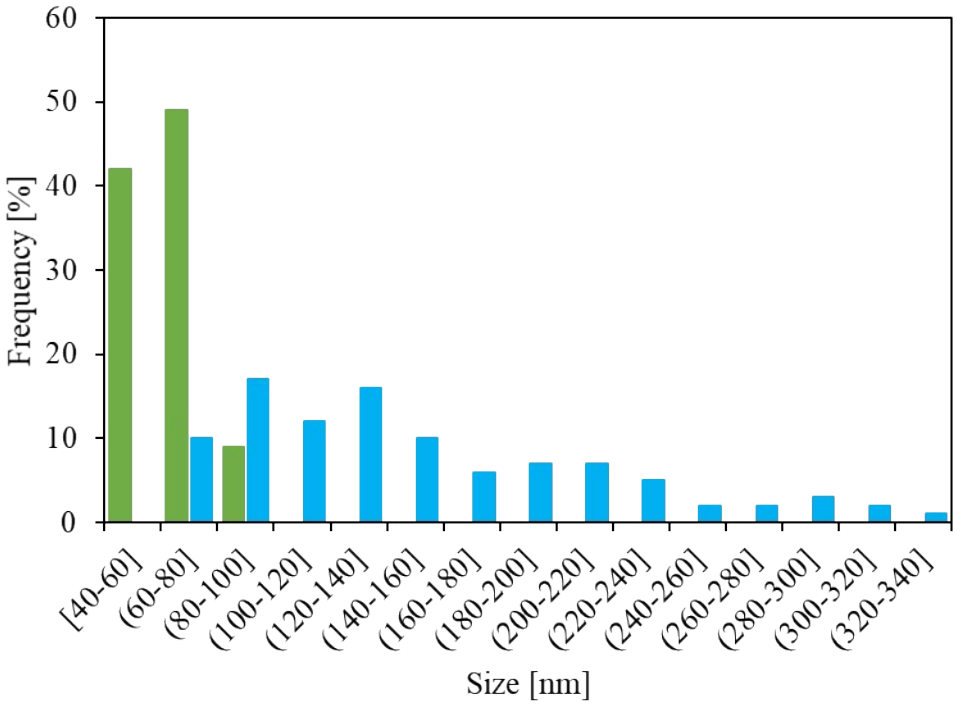

Figure S3. Particle size distribution histograms measured from the TEM images of CaSyr-1 prepared in 10 mL (green, 1:80 reactants:solvent molar ratio) and 1 mL (blue, (1:8 reactants:solvent molar ratio) of EtOH.

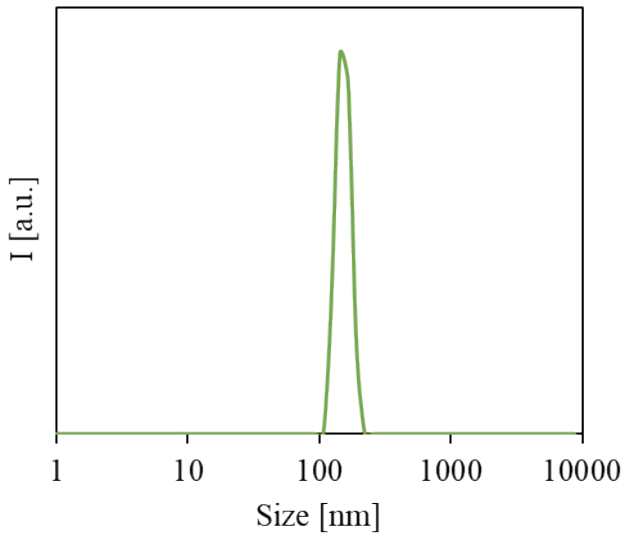

Figure S4. Particle size distribution of CaSyr-1 under suspension according to DLS.

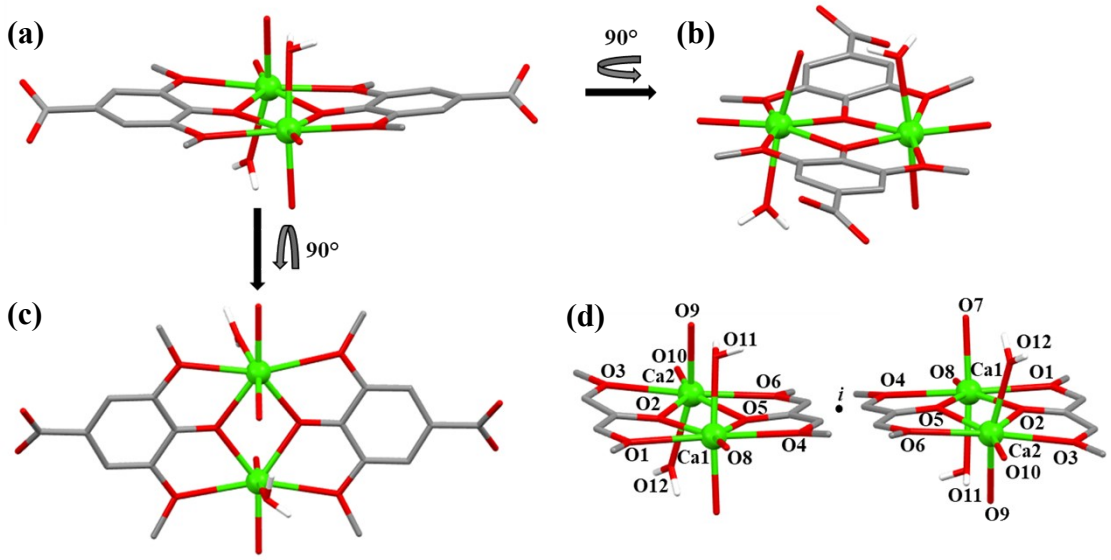

Figure S5. Dimeric unit of CaSyr-1: (a,b,c) observed from different angles, and (d) center of inversion between the interconnected dimers.

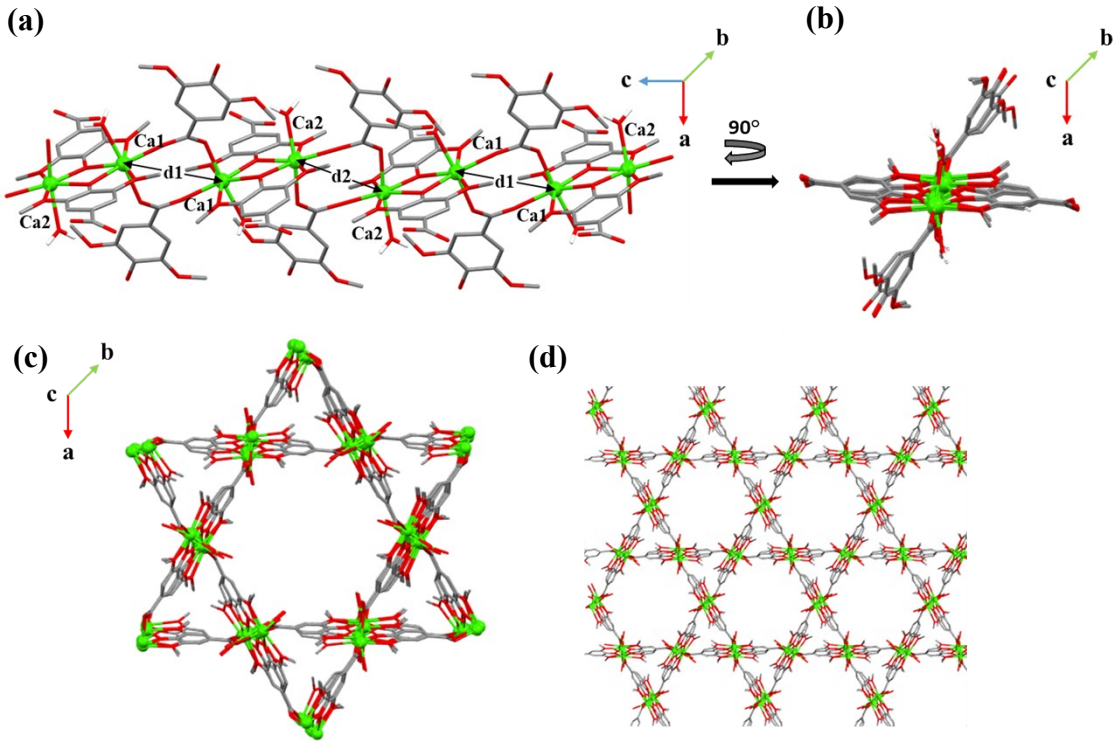

Figure S6. Chains formed after dimmer connection in: (a) –{[Ca2Ca1]-[Ca1Ca2]}$_n$- fashion (b), visualized from c axis; (c) chains interconnection forming triangular and hexagonal prisms, and (d) resembling Kagome lattice.

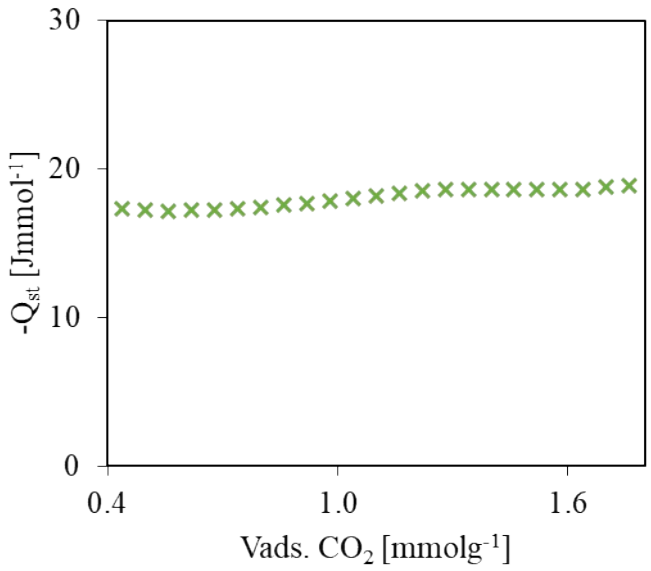

Figure S7. CO_2 enthalpy of adsorption (Q_{st}) of CaSyr-1.

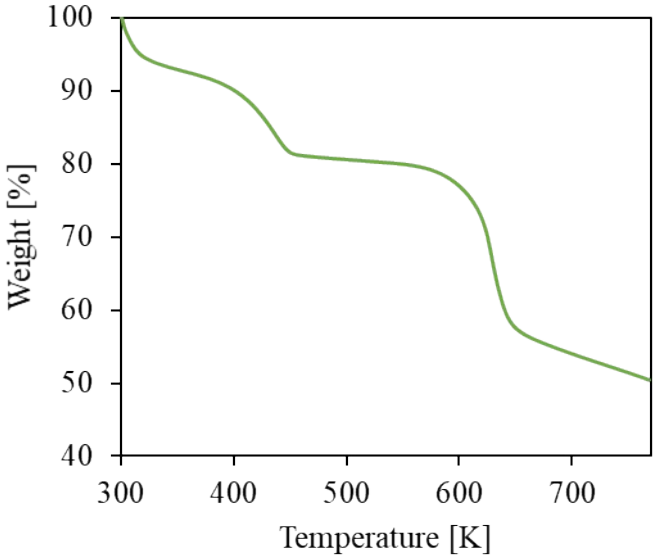

Figure S8. Thermogravimetric analysis of CaSyr-1 under N_2.

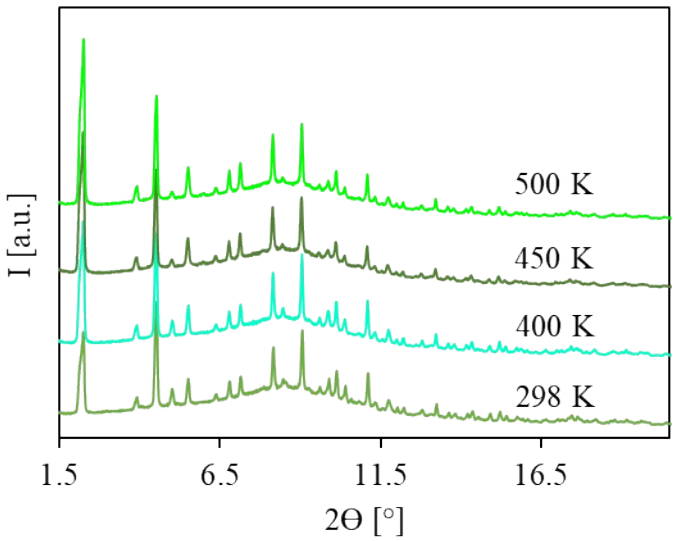

Figure S9. Variable-temperature PXRD (VTPXRD) of CaSyr-1 up to 500 K.

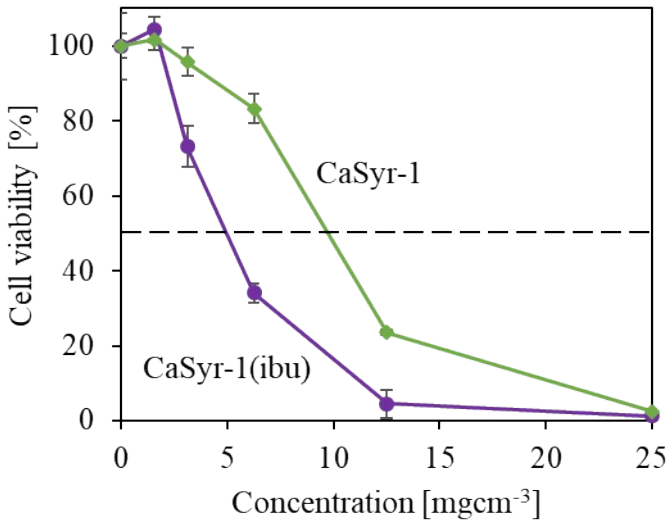

Figure S10. Cytotoxicity results of CaSyr-1 and CaSyr-1(ibu).

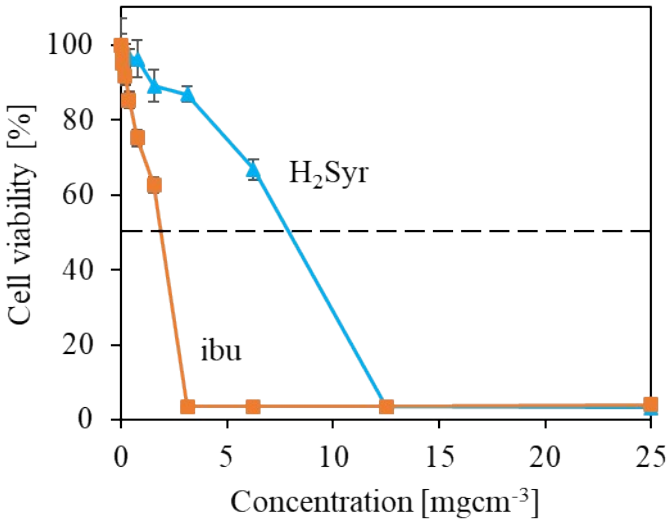

Figure S11. Cytotoxicity results of syringic acid and ibuprofen.

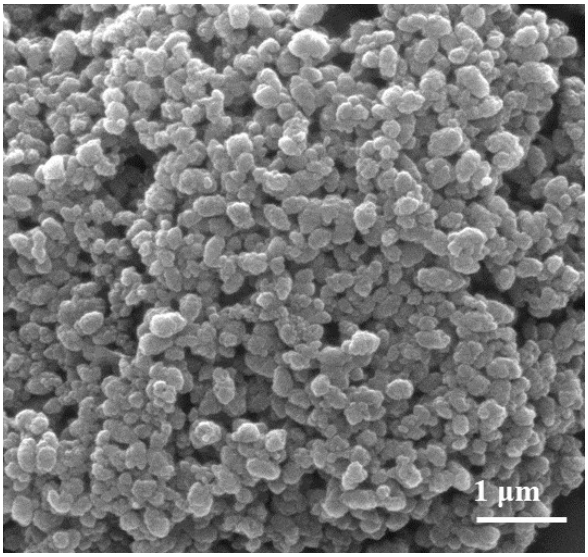

Figure S12. SEM image of CaSyr-1(ibu).

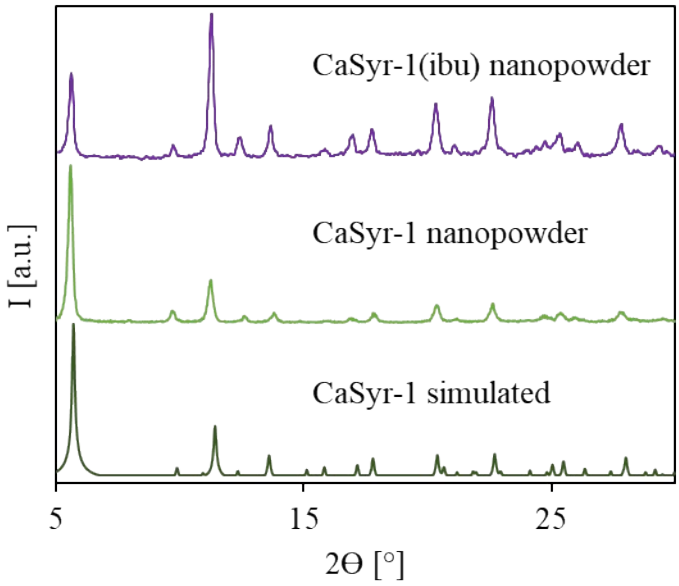

Figure S13. PXRD pattern of CaSyr-1(ibu) nanopowder compared to CaSyr-1 nanopowder (1:80 reactants:EtOH molar ratio) and the simulated pattern from single crystal structural data.

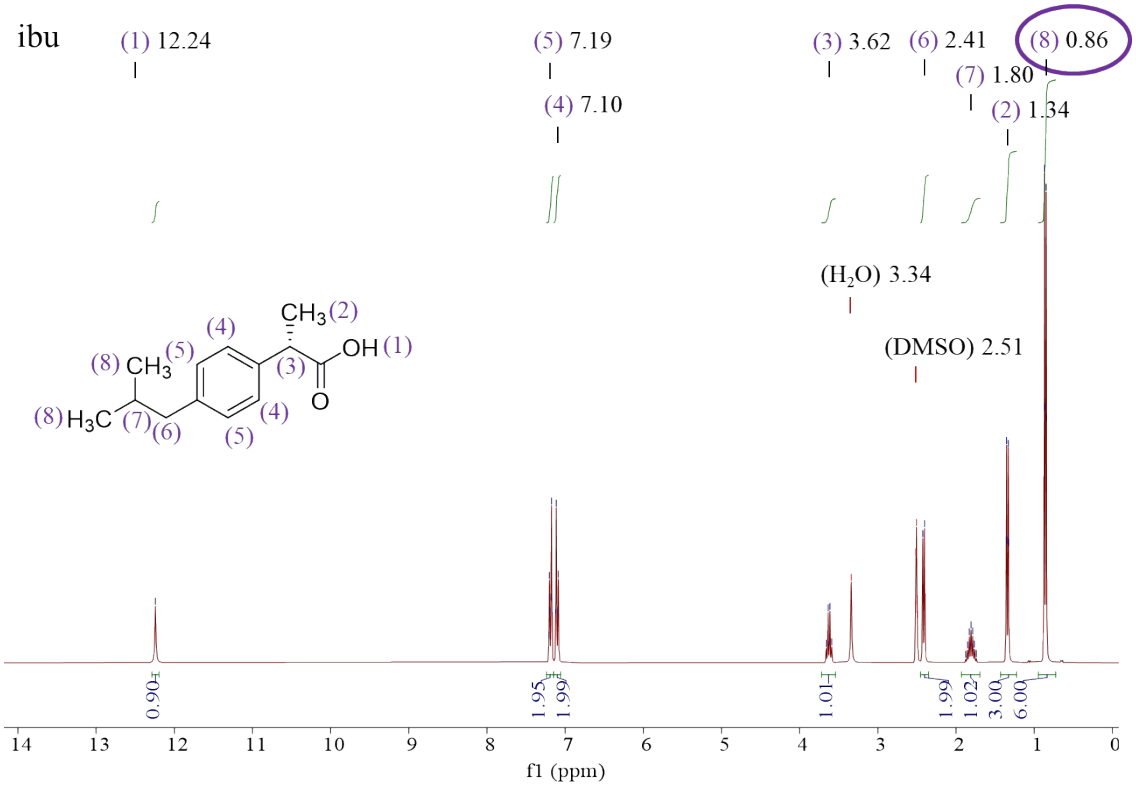

Figure S14. ^{1}H-NMR of (S)-(+)-ibuprofen.

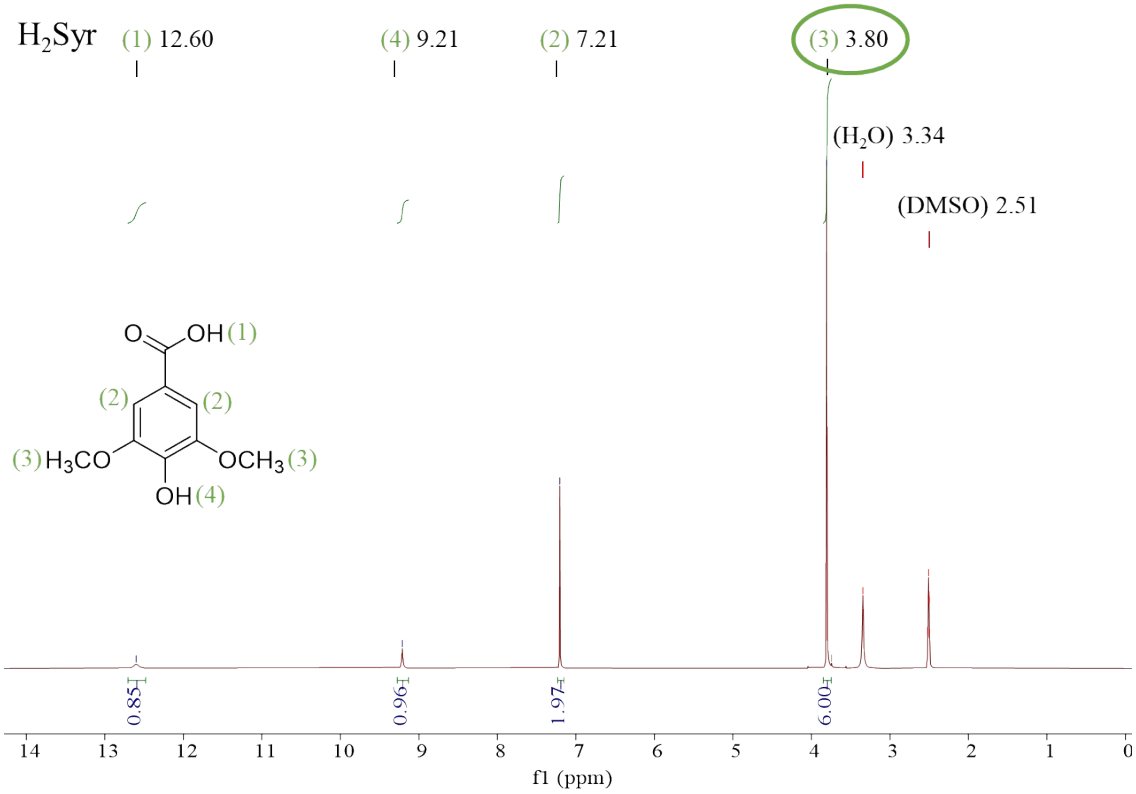

Figure S15. ^{1}H-NMR of syringic acid.

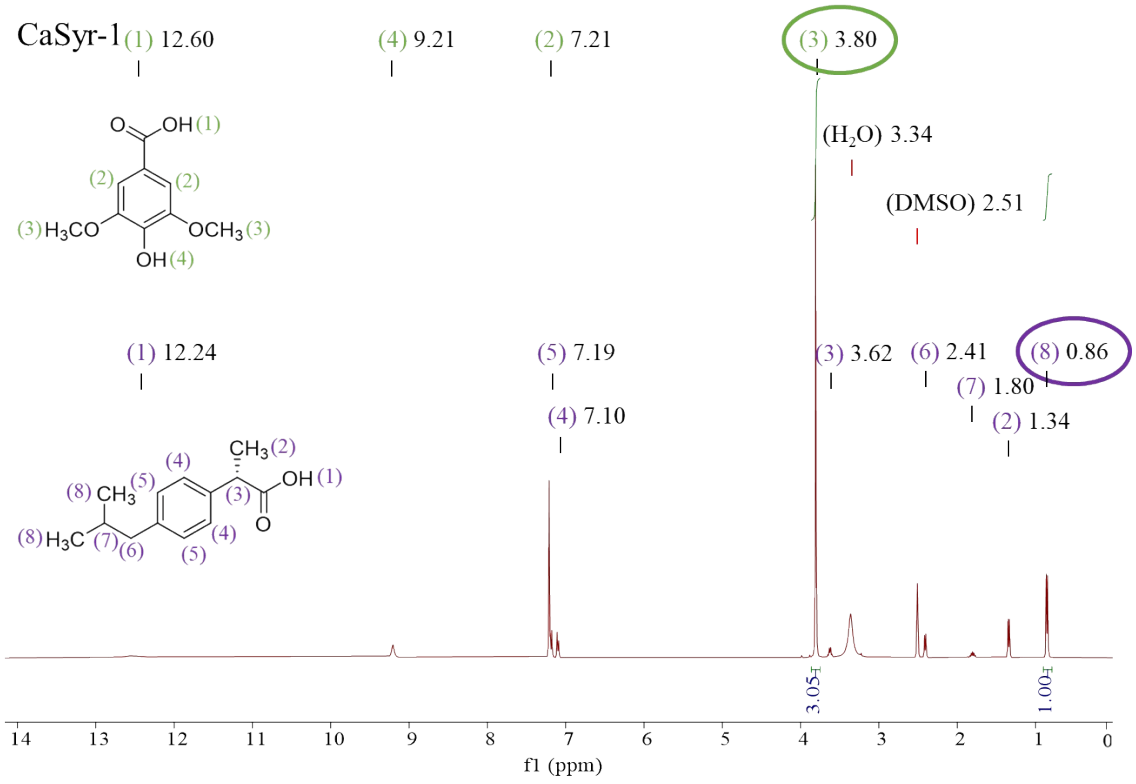

Figure S16. ^{1}H-NMR of CaSyr-1(ibu) after HF treatment and filtration.

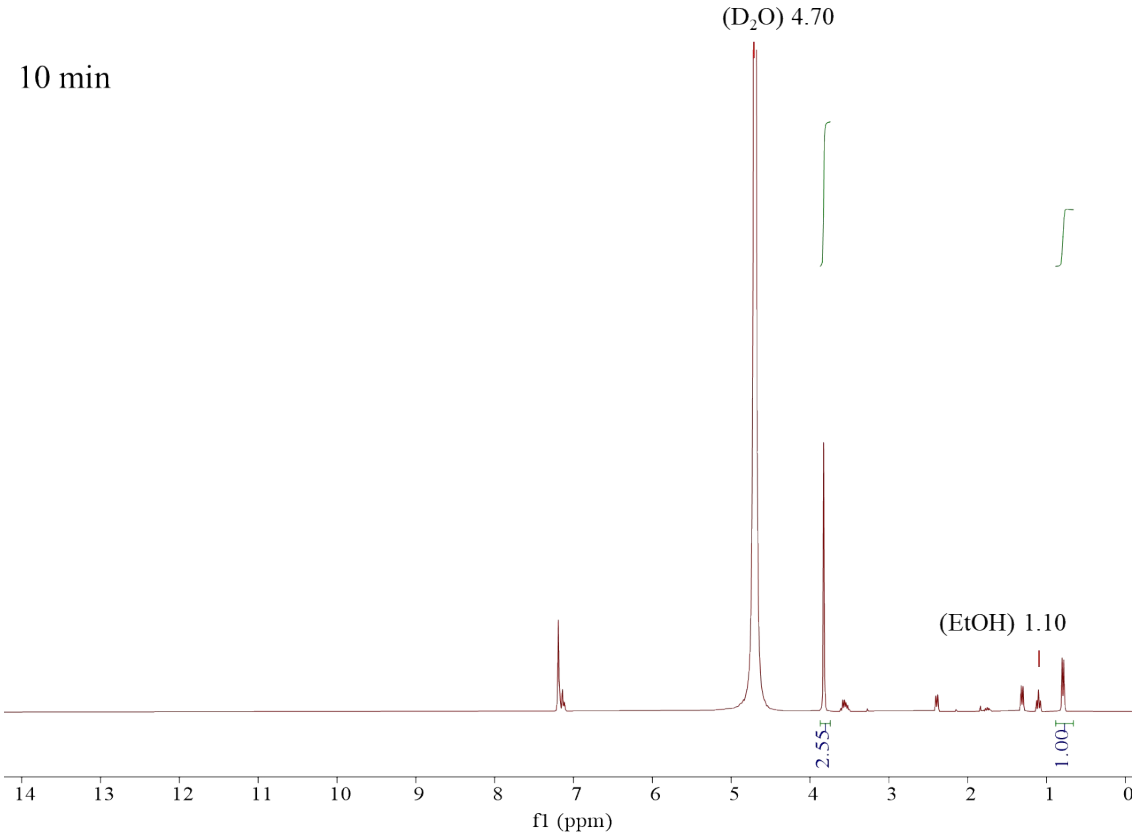

Figure S17. [1]H-NMR of CaSyr-1(ibu) release after 10 min of exposure to PBS medium.

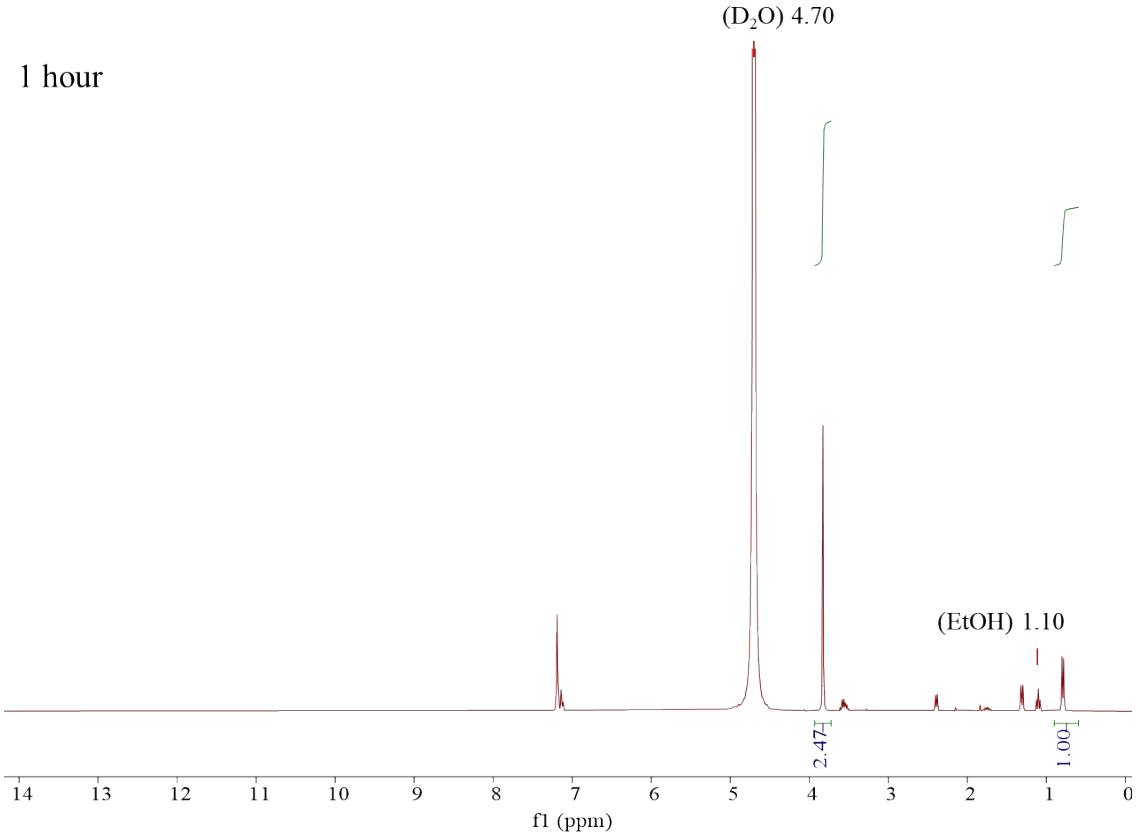

Figure S18. [1]H-NMR of CaSyr-1(ibu) release after 1 hour of exposure to PBS medium.

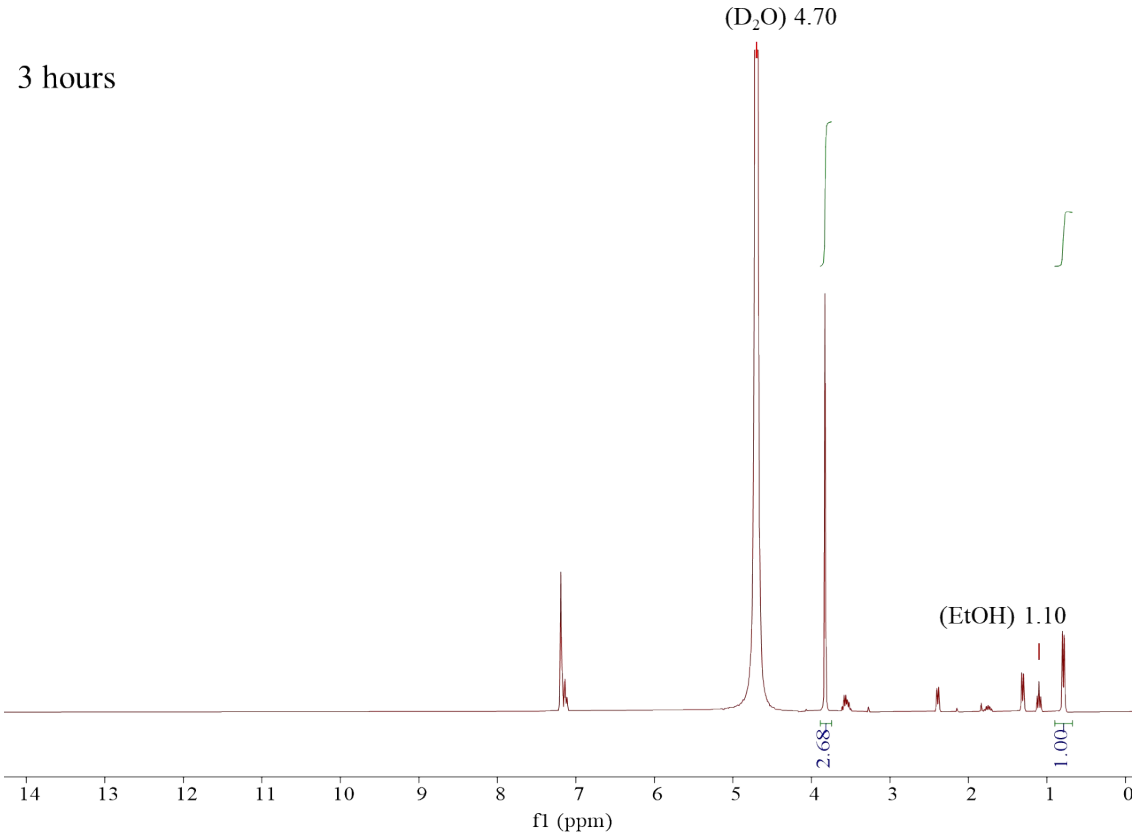

Figure S19. ^{1}H-NMR of CaSyr-1(ibu) release after 3 hour of exposure to PBS medium.

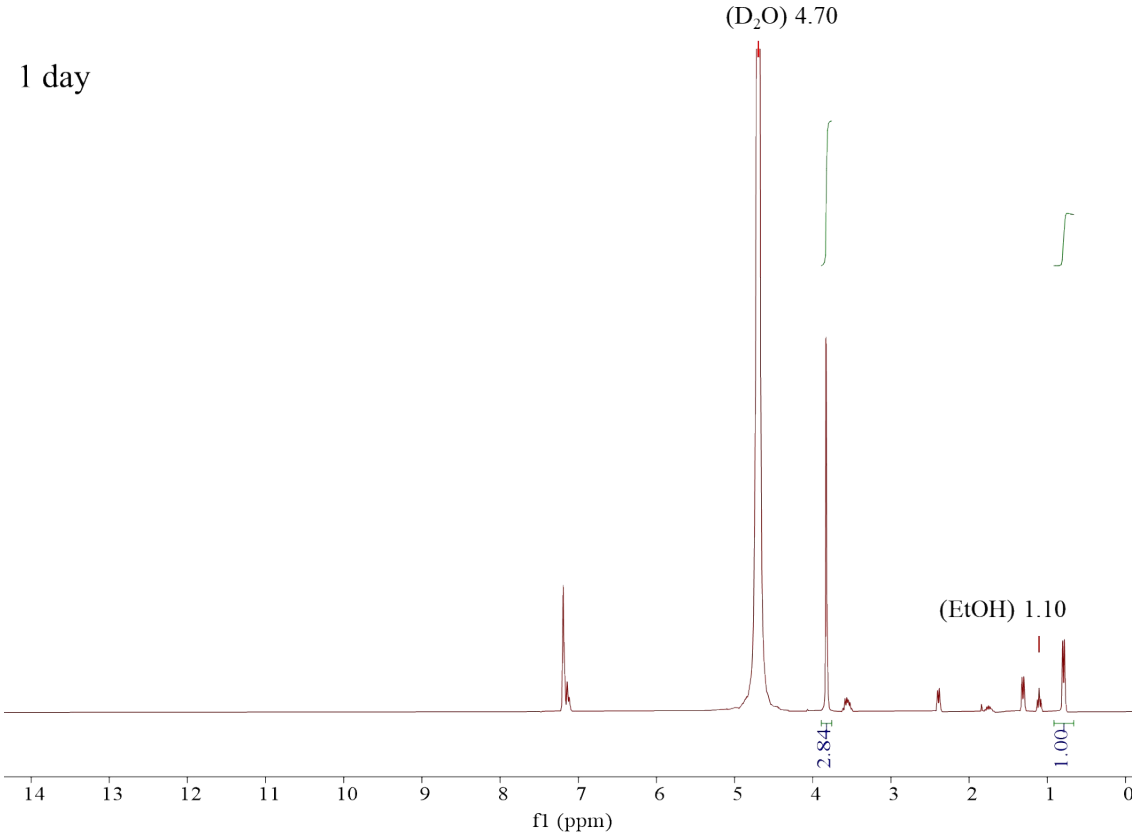

Figure S20. ^{1}H-NMR of CaSyr-1(ibu) release after 1 day of exposure to PBS medium.

Tables

Table S1. Elemental analysis of CaSyr-1 obtained in the synthesis performed with 1:80 reactantsts:solvent molar ratio.

Material	Calculated [%]		Experimental [%]		Ratio
	Carbon	Hydrogen	Carbon	Hydrogen	Ca:Syr:H_2O
CaSyr-1	42.52	3.96	42.19	3.92	1:1:1

Table S2. Calcium-based MOFs tested for CO_2 adsorption.

Ca-based MOF	CO_2 uptake [mmolg^{-1}]	Conditions T [K] / P [kPa]	Reference
CaSyr-1	3.7	273 / 100	This work
	2.4	298 / 100	
	1.8	313 / 100	
Ca-5TIA-MOF	1.12	298 / 100	S1
MUT-1	0.97	298 / 100	S2
CaBTB	1.98	298 / 100	S3
Ca(SDB)	1.04	273 / 100	S4

Table S3. Crystallographic data for CaSyr-1 determined by single crystal XRD.

Empirical formulae	C_{18} H_{20} Ca_2 O_{12} [2(H_2 O) 2(C_3 H_7 N O)]
Formula weight	690.72
T [K]	100(2)
Wavelength [Å]	0.72932
System, space group	Trigonal, $R\bar{3}$
a [Å]	30.963(2)
b [Å]	30.963(2)
c [Å]	16.953(1)
α [º]	90
β [º]	90
γ [º]	120
V [Å^3]	14075(2)
Z	18
*D*calc [g cm^{-3}]	1.467
μ [mm^{-1}]	0.469
F(000)	6552.0
Crystal size [mm^3]	42
hkl ranges	-42≤h≤42 -42≤k≤42 -23≤l≤23
2Θ range [º]	1.458 to 30.427
Reflections collected/unique/[R_{int}]	83456/8717/[R_{int} = 0.0390]
Completeness	99.4%
Refinement method	Full matrix least-squares on $\|F\|^2$
Data/restrains/parameters	8717/ 0 / 295
Goodness of fit (GOF) on $\|F\|^2$	1.061
Final *R* indices [I>2σ(I)]	R1 = 0.0336, wR2 = 0.1001
R indices (all data)	R1 = 0.0360, wR2 = 0.1018
Largest Diff. peak and hole [e Å^{-3}]	0.451 and -0.494

Table S4. Selected bond distances in CaSyr-1.

Bond	**Distance [Å]**
Ca1-O1	2.649(1)
Ca1-O2	2.303(1)
Ca1-O4	2.555(1)
Ca1-O5	2.343(2)
Ca1-O7	2.302(2)
Ca1-O8	2.261(1)
Ca1-O11	2.388(2)
Ca2-O2	2.327(1)
Ca2-O3	2.540(1)
Ca2-O5	2.308(1)
Ca2-O6	2.675(2)
Ca2-O9	2.378(2)
Ca2-O10	2.273(1)
Ca2-O12	2.407(2)

Table S5. Selected bond angles in CaSyr-1.

Objects	Angle [º]
O1-Ca1-O2	64.07(4)
O2-Ca1-O5	69.58(5)
O4-Ca1-O5	65.52(5)
O2-Ca2-O3	65.77(4)
O2-Ca2-O5	69.79(5)
O5-Ca2-O6	63.61(5)
Ca1-O2-Ca2	110.28(5)
Ca1-O5-Ca2	109.51(6)

References

S1. A. Mallick, E. M. Schön, T. Panda, K. Sreenivas, D. Díaz, R. Banerjee, Fine-tuning the balance between crystallization and gelation and enhancement of CO_2 uptake on functionalized calcium based MOFs and metallogels, *J. Mater. Chem.*, 2012, **22**, 14951-14963.

S2. R. K. Alavijeh, K. Akhbari, J. White, Solid−Liquid Conversion and Carbon Dioxide Storage in a CalciumBased Metal−Organic Framework with Micro- and Nanoporous Channels, *Cryst. Growth Des.*, 2019, **19**, 7290−7297.

S3. K. Noh, N. Ko, H. J. Park, S. Park, J. Kim, Two porous metal–organic frameworks containing zinc–calcium clusters and calcium cluster chains, *CrystEngComm*, 2014, **16**, 8664-8868.

S4. D. Banerjee, Z. Zhang, A. M. Plonka, J. Li, J. B. Parise, A Calcium Coordination Framework Having Permanent Porosity and High CO2/N2 Selectivity, *Cryst. Growth Des.* 2012, **12**, 2162−2165.